https://doi.org/10.70844/ijas.2025.1.18

Innovative Journal of Applied Science

Research Article

IJAS-25-047

Kinetic Analysis of Reduction Reaction of MnO from High Carbon Ferromanganese Slag using Fractional Differential Equations (FDE)

Kim UnDok[1], Kim MyongJae[*1], Ju IlChol[2]

[1]*Department of Chemical Engineering, Kimchaek University of Technology, Pyongyang, North Korea*

[2]*Department of Chemical Engineering, State Academy of Science, Pyongyang, North Korea*

Corresponding Author: Kim MyongJae, Department of Chemical Engineering, Kimchaek University of Technology, Pyongyang, North Korea, E-mail: kmj0703@126.com

Received date: 03 February, 2025, **Accepted date:** 14 April, 2025, **Published date:** 21 April, 2025

Citation: UnDok K, MyongJae K, IlChol J (2025) Kinetic Analysis of Reduction Reaction of MnO from High Carbon Ferromanganese Slag using Fractional Differential Equations (FDE). Innov J Appl Sci 2(2): 18.

Abstract

In this paper, a kinetic model for the reduction process by solid carbon of MnO in high-carbon ferromanganese slags using Fractional Differential Equations (FDE) was developed, the relationship between fractional order, fractional rate constant and temperature was determined and the accuracy of the fractional order model was verified. The fractional order *q* is 0.892, 0.808 and 0.522, at 1,450 ℃, 1,500 ℃ and 1,600 ℃ respectively and the fractional rate constant k_q 1.176E-03, 2.856E-03 and 3.477E-02. A linear relationship exists between the fractional order and the temperature and an exponential relationship exists with the fractional rate constant. Comparing the conversion factors calculated from the FDE and previous model with the experimental values, the RMSE were 0.005 and 0.029, respectively and the r^2 0.999 and 0.980. This means the FDE model is more accurate. The apparent activation energy of the MnO reduction process calculated using the model was 181.1 kJ/mol.

Keywords: Fractional Differential Equation (FDE), Fractional rate constant, MnO reduction, Kinetics, Conversion factor

Introduction

Manganese is an important alloying element indispensable in the metallurgical industry and it is widely deposited in the form of oxides in nature. The studies on the reduction reaction of manganese oxides in the production of metallic manganese or ferromanganese from these manganese raw materials are of great importance and thermodynamic and kinetic studies on the reduction reaction of manganese oxides have been carried out by many researchers [1-3]. In particular, several kinetic models describing the carbothermic reduction reaction of MnO proposed and experimentally examined [4,5]. The reduction of MnO by solid carbon is represented by the following reactions.

$$(MnO)+C=Mn+CO(g) \quad (1)$$

Shibata E, et al., evaluates the reduction rate of MnO in CaO-SiO_2-CaF_2-MnO-FeO slags and suggests that the reaction is rate-controlled by mass transfer in the metallic phase [6]. In Rankin WJ, et al., considered solid carbon as a porous material and performed a kinetic study of manganese oxide reduction reaction, revealing that the rate-limiting step of the reaction is the diffusion-transfer step of the gas to the reaction zone [7]. In addition, Berg KL, et al., considered the reduction reaction of MnO in the temperature range of 700~1,100 ºC and considered that the reaction was controlled by diffusion outside the reaction zone of the product [8]. Jamieson BJ, et al., studied the reduction reaction of MnO in MnO-SiO_2-CaO-Al_2O_3-based slag by FeSi and reported that the reaction was controlled by the migration of Si in the metal phase and the migration of MnO in the slag phase [9]. In Safarian J, et al., carried out kinetic research and proposed a kinetic model for the reduction reaction by solid carbon of MnO in high-carbon ferromanganese slag [4]. The apparent activation energy of the reduction reaction of MnO calculated by this is 227.7kJ/mol.

However, there are some errors in the calculation and experimental results in the models proposed by the previous authors and no studies have yet applied the fractional order in the kinetic modeling of the reduction reaction of MnO by solid carbon.

Accurate description of the rate at which a chemical reaction takes place is a fundamental task of chemical kinetics. Many researchers have been interested in developing accurate mathematical models to describe chemical kinetics. Most of them have used differential equations of integer order for mathematical modeling of chemical reactions. In general, however, real objects can be considered as systems of fractional order (0.8, 0.9...), even though in some systems the differential order is very close to the integer order (first order, second order). In recent years, fractional kinematics theory has been widely used to describe phenomena in control theory, electrochemical processes, viscoelastic materials, heat conduction and chaos [10-20]. In particular, in the last few decades, modeling methods of chemical reactions using fractional-order operators have continued to be generalized and developed. Ghaemi F, et al., developed a fractional

kinetic equation model to predict the concentration of xylose with time in the hemicellulose hydrolysis reaction to increase the computational accuracy and an example of this can be found in a study using the fractional calculation method for the flotation process in Vinnett L, et al., [21,22].

In this paper, the kinetic research of the reduction reaction of MnO in high-carbon ferromanganese slags by solid carbon were carried out using fractional differential equations, the fractional order and fractional order were calculated, the fractional order and temperature dependence of the rate constant were determined and the apparent activation energy was calculated.

FDE Modeling

Model developing

Under the assumption that the rate-limiting step of the reaction is the interaction between reactants at the interface, Safarian et al. proposed the following differential equation for kinetically considering the reduction reaction of MnO in high-carbon ferromanganese slag by solid carbon [8].

$$-\frac{dC_{MnO}}{C_{MnO}^{\gamma}} = k_m \frac{A_t}{V_s} dt \tag{2}$$

where, CMnO- the concentration of MnO in the slag phase, %; γ-reaction order VS-slag volume, m3; At- the total reaction interfacial area, m2; km-mass transfer coefficient m/s.

Eq. (2) is the basic differential equation representing the carbothermic reduction of MnO in a graphite crucible. However, since the ratio of the area of the interface to the slag volume, At/Vs depends on the slag density and CMnO and it is not the first-order variable separation equation. In the general case, it has to be solved numerically for various initial and boundary conditions. However, since the At/Vs ratio did not change significantly during the isothermal reduction, Eq. (2) could be considered as the first-order variable separation equation.

According to Safarian et al., the experimental data for the reference system are best represented by the first-order reaction (γ=1), so Eq. (2) is represented by Eq. (3) [8].

$$-\frac{dC_{MnO}}{C_{MnO}} = k_m \frac{A_t}{V_s} dt \tag{3}$$

Safarian J, et al., the authors calculated the MnO concentration with time using the proposed model and compared the experimental values with a significant error [4]. In order to overcome this shortcoming, a modeling method using FDE is proposed.

If we set k as the rate constant of the reaction and perform the variable transformation using the conversion factor (α), Eq. (3) is as follows.

$$\frac{d\alpha}{dt} = k \cdot \left(\frac{C_{MnO}^0}{C_{MnO}^0 - C_{MnO}^{eq}} - \alpha \right) \tag{4}$$

Where $k = k_m \frac{A_t}{V_s}$, $\alpha = \frac{C_{MnO}^0 - C_{MnO}}{C_{MnO}^0 - C_{MnO}^{eq}}$

By replacing the first derivative with the fractional derivative of Caputo, the fractional differential equation (5) is obtained from the first derivative equation (4).

$${}^{c}D^{q}\alpha(t) = \frac{d^q\alpha}{dt^q} = k_q \cdot \left(\frac{C_{MnO}^0}{C_{MnO}^0 - C_{MnO}^{eq}} - \alpha \right) \tag{5}$$

α(0)=0, 0<q<1

where q-fractional order; k_q-fractional rate constant.

Substituting $C_{MnO}^0 = 45\%$ and $C_{MnO}^{\infty} = C_{MnO}^{eq} = 15\%$ for Eq. (5), we could obtain the fractional differential Eq. (6).

$${}^{c}D^{q}\alpha(t) = \frac{d^q\alpha}{dt^q} = k_q \cdot (1.5 - \alpha) \tag{6}$$

α(0)=0, 0<q<1

Hence, we can calculate the rate of conversion with time as a solution of the linear fractional differential Eq. (6).

Solution of FDE

One of the most common fractional differential operators used in the scientific and technological fields is the Caputo Fractional Derivative (CFD). That is,

$${}_{a}^{C}D_t^q x(t) = \frac{1}{\Gamma(n-q)} \int_a^t (t-\tau)^{n-q-1} x^{(n)}(\tau) d\tau \tag{7}$$

where n means [q]+1 (n is the smallest integer bigger than q) and Γ is the gamma function. That is,

$$\Gamma(z) = \int_0^{\infty} t^{z-1} e^{-t} dt \ , \ z>0 \tag{8}$$

Let us first consider the following Eq. (9),

$$a_1 x^q(t) + a_0 x(t) = 1 \tag{9}$$

x(0)=0

where a_0, a_1 are arbitrary constants.

An analytical solution to the Eq. (9) is presented in 23. Podlubny I and Podlubny I [23,24]. If q=1, the solution is represented by an exponential function (Eq. (10)) and if q≠1, by a Mittag-Leffler expression (Eq. (11)).

$$x(t) = \frac{1}{a_0} \left(1 - e^{-\frac{a_0}{a_1} t} \right) \tag{10}$$

$$x(t) = \frac{1}{a_1} t^q E_{q,q+1} \left(-\frac{a_0}{a_1} t^q \right) \tag{11}$$

Where $E_{\alpha,\beta}(z)$ is a function of Mittag-Leffler with two parameters.

$$E_{\alpha,\beta}(z)=\sum_{k=0}^{\infty}\frac{z^k}{\Gamma(\alpha k+\beta)} \quad (12)$$

In our case, $a_1=\frac{1}{1.5\cdot k_q}$, $a_0=\frac{1}{1.5}$, so the basic fractional differential equation (6) can be written as:

$$\alpha(t)=1.5.k_q.t^q.E_{q,q}+1\ (-k_q t^q) \quad (13)$$

Once q and k_q are given, we can find the relationship between conversion factor α and t from Eq. (13).

Estimation of parameters

Estimation of the fractional order and fractional rate constants in the FDE model was determined by iterative calculation using Matlab software, until the sum of the squares of the calculated and experimental errors (Eq. (14)) was less than 0.005.

$$S=\sum_{i=1}^{N}\left(\alpha_{cal}\left(q,k_{q,}t(i)\right)-\alpha_{obs}\left(t(i)\right)\right)^2 \quad (14)$$

Where α_{cal} is calculated as the solution (Eq. (13)), α_{obs} is the observed value during the experiment and N is the number of observed values.

For the calculation of the Mittag-Leffler function, the Mittag-Leffler procedure and the Matlab nonlinear least squares regression analysis (nlinfit command) were used.

We used the Root-Mean-Square Error (RMSE) and the coefficient of determination (r^2) as indicators to evaluate the accuracy of the model. These indices are calculated by the following equation.

$$RMSE=\sqrt{\frac{\sum_{i=1}^{N}\left(\alpha_{cal,i}-\alpha_{obs,i}\right)^2}{N}} \quad (15)$$

$$r^2=1-\frac{\sum_{i=1}^{N}\left(\alpha_{obs,i}-\alpha_{cal,i}\right)^2}{\sum_{i=1}^{N}\left(\alpha_{obs,i}-\overline{\alpha}_{obs}\right)^2} \quad (16)$$

Where α_{obs} , i is the ith experimental value, α_{cal} , i the ith predicted value and $\overline{\alpha}_{obs}$ the algebraic mean of the experimental values.

Validation and Discussion of the FDE model

Validation of the FDE model

In the validation of the model, the experimental data presented in Safarian J, et al., were used [4]. The fractional order and fractional order constants with temperature determined using the estimation method mentioned above are shown in Table 1 and Figure 1.

Temperature, °C	1,450	1,500	1,600
q	0.892	0.808	0.522
kq	1.18E-03	2.86E-03	3.48E-02

Table 1: The parameters of the fractional model.

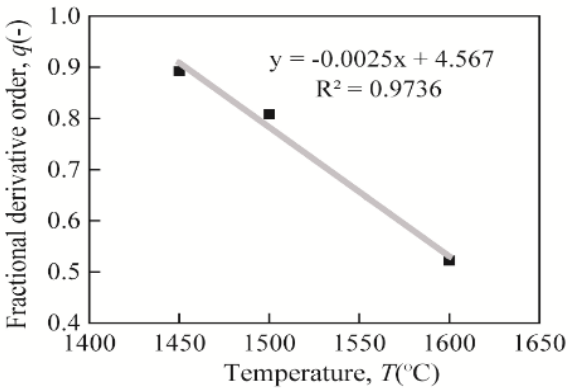

Figure 1: Relationship between the temperature T and fractional derivative order q.

It can be seen from Table 1 and Figure 1 that as the temperature increases, the order of the fractional derivative decreases linearly. In other words, it can be seen that the more pronounced the fractional mechanical properties are as the temperature increases.

On the other hand, the comparison of the FDE model calculations with the experimental data with the model proposed in Safarian J, et al., is shown in Figure 2, Figure 3 also shows the comparison between the predicted and experimental MnO concentrations calculated from the model at different temperatures [4].

From Figure 2 and Figure 3, it can be seen that the FDE model is more accurate because the calculation results using the FDE model are more approximate to the experimental results compared to the model proposed in Safarian J, et al., [4].

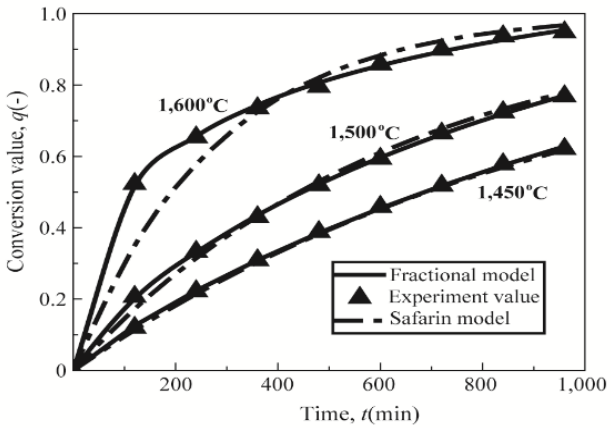

Figure 2: Relationship between conversion value and time.

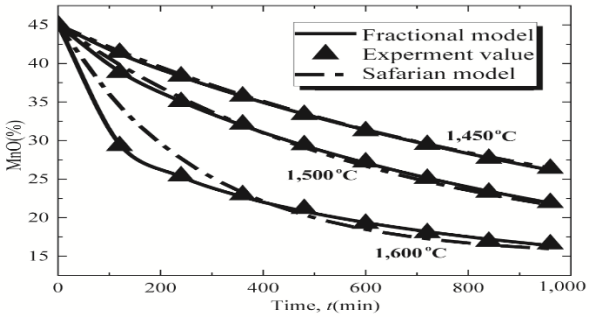

Figure 3: Relationship between MnO concentration and time.

In order to quantitatively compare the accuracy of the FDE model compared to the model proposed in Safarian J, et al., the RMSE and r^2 calculated results are presented in Table 2 [4].

		1,450	1,500	1,600	average
RMSE	Safarian J, et al.,	0.005 8	0.015 9	0.065 4	0.029 0
	fractional model	0.003 6	0.003 4	0.007 0	0.004 7
r^2	Safarian J, et al.,	0.999 2	0.995 6	0.946 3	0.980 4
	fractional model	0.999 7	0.999 8	0.999 4	0.999 6

Table 2: Accuracy comparison between Safarian J, et al., and fractional model [4].

From Table 2, it can be seen that the FDE model is more accurate compared to the model proposed in Safarian J, et al., [4].

The higher accuracy of the FDE model can be attributed to the fact that the model proposed in Safarian J, et al., has one parameter, whereas the FDE model has two parameters, fractional derivative order and fractional order constant.

Fractional rate constant equation

In order to consider the relationship between the fractional order and the temperature, the fractional order and the fractional order coefficient along the fractional order at different temperatures were calculated and the results are shown in Figure 4.

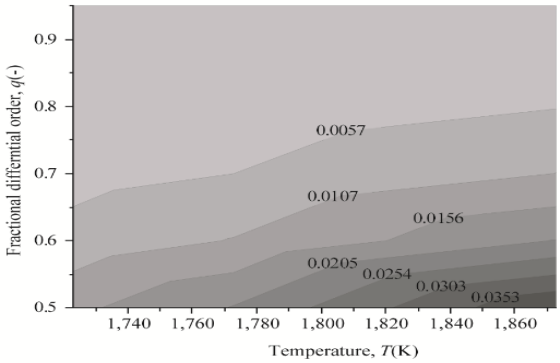

Figure 4: Fractional differential order with Fractional order and temperature.

From the calculated values of the fractional rate constant with temperature and fractional order of Figure 4, the relationship between fractional order q and ln k_q at constant temperature is shown in Figure 5.

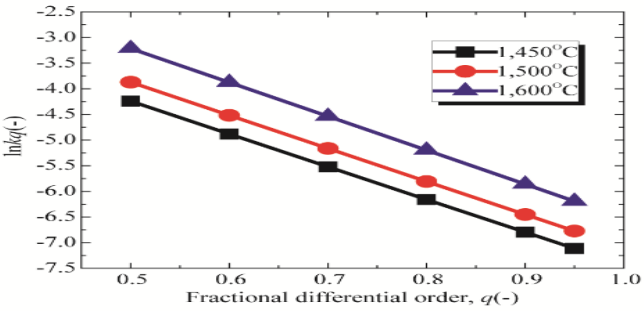

Figure 5: Relationship between q and ln k_q.

As can be seen from Figure 5, there exists a clear linear relationship between q and ln k_q and the lines are almost parallel. This means an exponential relationship between q and k_q when the temperature is constant.

$$k_q \propto e^{\lambda q} \tag{17}$$

where λ is the regression coefficient of the q-lnkq line.

On the other hand, using the data in Figure 4, the relationship between the fractional conductivity constant and temperature was considered.

Generally, temperature dependence of the first order rate constant is usually expressed by the Arrhenius equation [25,26].

$$\ln k = \ln A - \frac{E_a}{RT} \tag{18}$$

where A is the exponential factor, R is the apparent activation energy, R is the gas constant and T is the absolute temperature.

The apparent activation energy, Ea can be obtained by a linear plot of lnk versus 1/T according to the Arrhenius equation. In the small temperature range where kinetic studies are carried out, it is reasonable to treat the activation energy as an approximate quantity independent of the temperature when the graph is linear [27,28].

And then, in order to clarify whether the fractional rate constant satisfies the Arrhenius equation as the first order rate constant, we analyzed the relationship between lnkq and 1/T (Figure 6).

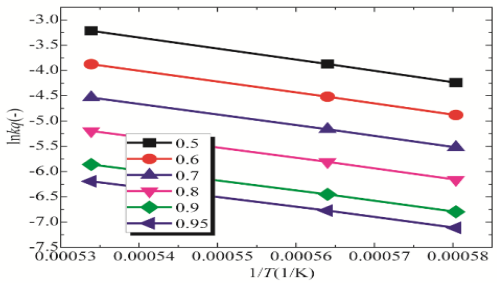

Figure 6: Relationship between lnkq and 1/T.

It can be seen from the figure that a linear relationship between lnkq and 1/T can be established.

$$k_q \propto e^{-\frac{c}{T}},\ c>0 \quad (19)$$

where c is the direction coefficient of lnkq - 1/T plot as a constant.

Taking into account Eq. (17) and Eq. (19), we assumed the structure of the fractional rate constant equation as follows.

$$k_q = A \cdot e^{\lambda q} \cdot e^{-\frac{E_a}{RT}} \quad (20)$$

The estimated parameters of Eq. (20) using nonlinear regression analysis method of the Matlab software are presented in Table 3.

Parameters	A	λ	E_a, kJ/mol
Values	1,19,645.20	-6.557	181.107

Table 3: Parameters of fractional continuation scheme.

Hence, Eq. (20) can be written as:

$$k_q = 119{,}645.2 \cdot e^{-6.557q} \cdot e^{-\frac{181{,}107}{RT}} = 119{,}645.2 \cdot e^{-6.557q-\frac{181{,}107}{RT}} \quad (21)$$

Conclusion

Using the FDE, a kinetic model for the MnO reduction reaction in high-carbon ferromanganese slag by solid carbon is proposed, the relationship between fractional order, fractional order, fractional order constant and temperature is analyzed and the accuracy of the new model is compared with the results of previous studies.

The values of conversion and MnO concentration in slag with time calculated by the proposed model are in good agreement with the experimental values.

The relationship between the fractional derivative order, the fractional rate constant and the temperature is clarified and a new fractional rate constant equation is proposed.

In the proposed model, the apparent activation energy of the reduction reaction was about 181.1 kJ/mol.

The results of the study can serve as a basis for rationalizing the high-carbon ferromanganese dissolution process, although the model's validation temperature range is limited to the range of 1,450-1,600 ℃. In the future, we will develop a more accurate model that can accurately simulate the high-carbon ferromanganese dissolution process in different temperature ranges and further work for practical applications.

Acknowledgments

We would like to thank the researchers and reviewers of Kim Chaek University of Technology, for their helpful comments and suggestions on this paper.

Data availability

Data sharing not applicable to this article as no datasets were generated or analyzed during the current study.

Conflicts of Interest

The authors declare that they have no conflict of interest.

References

1. Suito H, Inoue R (1984) Thermodynamics considerations on manganese equilibria between liquid iron and FetO-MnO-MOx (MOx=PO2.5, SiO2, AlO1.5, MgO, CaO) slags, Transctions ISIJ (24): 301-307. [Crossref] [GoogleScholar]
2. Li H, Morris AE, Robertson DGC (1998) Thermodynamic model for MnO-containing slags and gas-slag-metal equilibrium in ferromanganese smelting. Metallurgical and Materials Transactions B (29): 1181-1191. [Crossref] [GoogleScholar]
3. Li SJ, Cheng GG, Yang L, Chen L, Yan QZ, et al. (2017) A thermodynamic model to design the equilibrium slag compositions during electroslag remelting process: Description and verification. ISIJ International 57: 713-722. [Crossref] [GoogleScholar]
4. Safarian J, Grong O, Kolbeinsen L, Olsen SE (2006) A process model for the carbothermic reduction of MnO from high carbon ferromanganese slag-the model. ISIJ International 46: 1120-1129. [Crossref] [GoogleScholar]
5. Safarian J, Tranell G, Kolbeinsen L, Tangstad M, Gaal S, et al. (2008) Reduction kinetics of MnO from high-carbon ferromanganese slags by carbonaceous materials in Ar and CO atmospheres, Metallurgical and Materials Transactions B 39: 702-712. [Crossref] [GoogleScholar]
6. Shibata E, Sun H, Mori K (1999) Kinetics of simultaneous reactions between liquid iron-carbon alloys and slags containing MnO. Metallurgical and Materials Transactions B, 30: 279-286. [Crossref] [GoogleScholar]
7. Rankin WJ, Wynnyckyj JR (1997) Kinetics of reduction of MnO in powder mixtures with carbon. Metallurgical and Materials Transactions B 28: 307-319. [Crossref] [GoogleScholar]
8. Berg KL, Olsen SE (2000) Kinetics of manganese ore reduction by carbon monoxide. Metallurgical and Materials Transactions B 31: 477-490. [Crossref] [GoogleScholar]
9. Jamieson BJ, Coley KS (2017) Kinetics of silicothermic reduction of manganese oxide for advanced high-strength steel production. Metallurgical and Materials Transactions B 48: 1613-1624. [Crossref] [GoogleScholar]
10. Manabe S (1961) The non-integer integral and its application to control systems. ETJ of Japan 6: 83-87. [GoogleScholar]
11. Axtell M, Bise EM (1990) Fractional calculus applications in control systems. In Proc. of the IEEE Nat. Aerospace and Electronics Conf., New York, 563-566. [Crossref] [GoogleScholar]
12. Vinagre BM, Podlubny I, Hernandez A, Feliu V (2000) Some approximations of fractional order operators used in control theory and applications. Fractional Calculus & Applied Analysis 3: 945-950. [GoogleScholar]
13. Bagley RL, Torvik PJ (1986) On the fractional calculus model of viscoelastic behavior. J Rheol 30: 137-148. [Crossref] [GoogleScholar]
14. Mainardi F (1995) Fractional diffusive waves in viscoelastic solids. ASME 93-97.
15. Heymans N, Bauwens J (1994) Fractal rheological models and fractional differential equations for viscoelastic behavior. Rheologica Acta 33: 210-219. [Crossref] [GoogleScholar]
16. Ichise M, Nagayanagi Y, Kojima T (1971) An analog simulation of non-integer order transfer functions for analysis of electrode processes. J Electron Chem Interfacial Electrochem 33: 253-265. [Crossref] [GoogleScholar]
17. Li C, Chen G (2004) Chaos and hyperchaos in the fractional-order Rössle equations. Physica A 341: 55-61. [Crossref] [GoogleScholar]
18. Ahmad WM, Sprott JC (2003) Chaos in fractional-order autonomous nonlinear systems. Chaos, Solitons & Fractals 16: 339-351. [Crossref] [GoogleScholar]
19. Povstenko YZ (2004) Fractional heat conduction equation and associated thermal stress, Journal of Thermal Stresses 28: 83-102. [Crossref] [GoogleScholar]

20. Podlubny I, Misanek J (1993) The use of fractional derivatives for solution of heat conduction problems. Proceedings of the 9th Conference on Process Control 270-273.
21. Ghaemi F, Yunus R, Ahmadian A, Salahshour S, Suleiman M, et al. (2013) Application of fuzzy fractional kinetic equations to modelling of the acid hydrolysis reaction, Abstract and Applied Analysis 19. [Crossref] [GoogleScholar]
22. Vinnett L, Alvarez-Silva M, Jaques A, Hinojosa F, Yianatos J (2015) Batch flotation kinetics: fractional calculus approach. Minerals Engineering 77: 167-171. [Crossref] [GoogleScholar]
23. Podlubny I (1994) The laplace transform method for linear differential equations of the fractional-order. The Academy of Science Institute of Experimental Physics 32. [Crossref] [GoogleScholar]
24. Podlubny I (1999) Fractional differential equations 340.
25. Gorenflo R, Loutschko J, Luchko Y (2002) Computation of the mittag-leffler function and its derivatives. Fractional Calculus and Applied Analysis 5(4): 491-518.
26. Khawam A, Flanagan DR (2006) Basics and applications of solid-state kinetics: A pharmaceutical perspective. Journal of Pharmaceutical Sciences 95: 472-498. [Crossref] [GoogleScholar]
27. Laidler KJ (1994) The development of the Arrhenius equation. Journal of Chemical Education 61: 494. [Crossref] [GoogleScholar]
28. Atanackovic TM, Stankovic B (2008) On a numerical scheme for solving differential equations of fractional order. Mechanics Research Communications 35: 429-438. [Crossref] [GoogleScholar]